Progress In Electromagnetics Research C, Vol. 109, 65–75, 2021

Triple-Band Circular Polarized Antenna for WLAN/Wi-Fi/Bluetooth/WiMAX Applications

Izzat Fatima[1, *], Aqsa Ahmad[2], Saqib Ali[3], Mudassir Ali[3], and M. Iram Baig[1]

Abstract—A planar geometry triple-band circularly polarized (CP) antenna is proposed for wireless applications. The antenna consists of rectangular strips on the upper surface along with rectangular slots on the ground plane. The 3 dB axial-ratio of the antenna is achieved through a reformed ground plane. Through the aid of these features, a small, compact wideband circularly polarized antenna is fabricated with an area of $25 \times 25 \times 1.02\,\mathrm{mm}^3$. The -10 dB impedance bandwidth of the proposed antenna is 8.2% (2.4–2.58 GHz), 33% (3.2–3.9 GHz), and 41.1% (5.2–7.8 GHz). While the 3 dB axial ratio bandwidth achieved by the proposed antenna is 89.7% (2.17–5.8 GHz). The designed antenna is suitable for wireless applications such as WiMAX, WLAN, ISM, Bluetooth, and Wi-Fi.

1. INTRODUCTION

With the rapid development of modern wireless communication systems, the demand for compact, small size, and low-cost broadband antennas is increasing day by day [1]. Recently, circularly polarized (CP) antennas for several wireless applications, especially for WLAN (2.4–2.48, 5.15–5.35, 5.725–5.825 GHz), WiMAX (2.5–2.69, 3.4–3.69, 5.25–5.85 GHz), Wi-Fi (2.4–2.485, 5.15–5.85 GHz), and Bluetooth (2.4–2.5 GHz), have received more attention than linearly polarized (LP) antennas [2]. CP antennas have performance advantages over LP antennas such as maximum intensity toward power reception, the reflectivity of sending and receiving signals in all planes, easier installation, opposition to unpleasant climate conditions, and alleviated multipath losses [3]. In recent years, monopole antennas along with the benefits of low profile, low cost, broad bandwidths, and simple structure have been extensively used. The main shortcoming of CP antennas is their bandwidth limitation and large size. To overcome these shortcomings, designing a small size, broadband CP antenna with wide axial ratio bandwidth (ARBW) becomes the utmost challenging task for researchers [4].

From the last few years, planar geometry monopole antennas have gained significant attention due to their simplified configuration, easy incorporation, and multiband operation capability. Various broadband antennas with planar geometry to improve AR bandwidth for different applications like GSM and WLAN, by keeping the size as small as possible, have been proposed in [5–26]. A triple-band G-shaped fed antenna has wide ARBW of 53.92% and impedance BW of 62.94% [5]. However, this antenna has a lower value of axial ratio than its bandwidth. In [6], In [6], a bent shaped feed with three slots in which one is T-shaped and two are inverted-L slots etched in ground plane is presented for wireless standards but has less BW. The antenna presented in [7] comprises a rectangular slot with a microstrip feed line. This antenna attains an IBW of 90.2%, and a 3 dB axial ratio is 40%. This antenna has better impedance bandwidth, but its axial ratio is less and does not cover its entire bandwidth. An inverted-L strip and a modified ground plane to realize CP operation are designed in [8]. The

Received 12 December 2020, Accepted 19 January 2021, Scheduled 26 January 2021
* Corresponding author: Izzat Fatima (ee.13.et.022@gmail.com).
[1] Electrical Engineering Department, University of Engineering and Technology, Taxila, Pakistan. [2] Electrical Engineering Department, University of Engineering and Technology, Lahore, Pakistan. [3] Research Institute for Microwave and Milli-meter Wave Studies, NUST, Islamabad, Pakistan.

-10 dB reflection coefficient bandwidths cover Wi-Fi, Bluetooth, and WLAN bands and partly cover the WLAN band. The 3 dB axial ratio covers 360 MHz (2.39–2.75 GHz) and 850 MHz (5.15–6 GHz) bands only. In [9], an L-shaped radiator with two opposite strips at corners of the ground plane covers 44% (2.35–3.66 GHz) and 70% (4.55–9.55 GHz) IBW with AR 35.9% (2.40–3.45 GHz), 44.0% (4.65–7.27 GHz), and 6.3% (8.13–8.66 GHz). A planar antenna is presented in [10] having IBW for the lower band is 9.7%, for middle band 11.3%, and the higher band is 60.2%. The axial ratio bandwidths are 4.9% at the lower band and 58.6% GHz at the upper band, respectively. The inverted F-shaped slotted radiating patch antenna with wide ARBW is presented in [11]. The IBW is 3.12 GHz 56% (2.25–4.0 GHz), with an axial ratio of 63.61% (2.38–4.60 GHz). Another antipodal Y-strip feed having slots in ground plane to enhance BW is presented by Nosrati and Tavassolian in [12], which covers impedance BW of 84% and ARBW 41%. However, this antenna covers good IBW, but its axial ratio is less. In [13], Yeung et al. proposed a circularly polarized antenna with axial ratio BW of 83.5% (4.3 GHz, 3–7.3 GHz) and S_{11} bandwidth of 92.6%. In [14], the proposed microstrip antenna is suitable for GSM and Wi-Fi/WLAN applications. Only the GSM band covers AR bandwidth. In [15], Jan et al. presents an open slot antenna in which the 3 dB axial ratio is 27%. A microstrip antenna with IBW 66.66% is presented in [16]. In [17], Mousavi et al. proposed an L-shaped monopole slot antenna which was fed by a C-shaped microstrip line. Its ARBW is 23%. Using two embedded stubs in the microstrip feed-line that excites a two-linked elliptical slot has led to an ARBW of 40% [18]. In [19], a compact, wideband directional CP antenna has been presented to achieve a wide IBW and AR. Liang et al. [20] propose an antenna loaded with modified stubs that achieved CP in dual bands, but the narrow axial ratio (AR) bandwidth is in the lower band. In [21], a circular split ring resonator has an IBW of 2726 MHz and less AR. In [22], an I-shaped patch is presented having an IBW of 115%, and AR is 56%, but still, it is not suitable for multiband applications, while a U-shaped patch is presented in [23] with less IBW having an ARBW of 18.91%. A hook-shaped antenna is presented in [24], having wide return loss and good axial ratio but is only suitable for ISM-band applications. Similarly, an array antenna and planar antenna with better IBW is presented in [25–27] but limited for Wi-Fi application. From the above literature analysis, the described antennas reveal a bit of complex structure or have narrow BW. To obtain wider CP bandwidth using slotted antennas with single-feed and compact size is a challenging task. Also, total impedance BW is not overlapped by the ARBW in these presented antennas. These are some major shortcomings of CP antennas.

In this paper, a simple, wide-band antenna is proposed which has slotted ground plane and enhanced F-shaped parasitic patch as shown in Fig. 1. The covered bandwidths of the proposed antenna are 8.2%

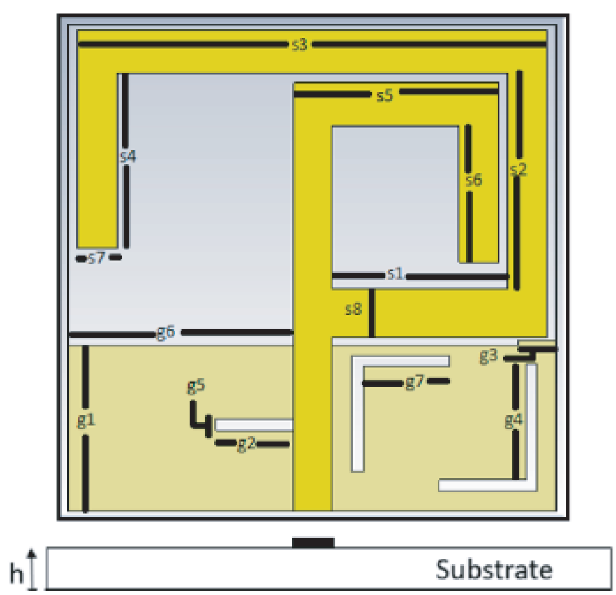

Figure 1. Schematic diagram of proposed antenna.

(2.4–2.58 GHz), 33% (3.2–3.9 GHz), and 41.1% (5.2–7.8 GHz), which have been designed to come across the necessities of wireless communication applications. The AR bandwidths are 89.7% (2.17–5.8 GHz). The antenna design gets the benefits of attaining a compact size, providing wide bandwidth, equivalent S_{11}, and AR bands. Simulated results of the proposed antenna are described and presented in detail.

2. ANTENNA DESIGN

The geometry of the designed antenna is shown in Fig. 1. The proposed antenna is fed by a 50 Ω feedline with a thickness of 1.02 mm and made on an FR-4 substrate (relative permittivity = 4.4). The size of the antenna is $25 \times 25\,\text{mm}^2$. The improved F shape antenna with rectangular strips is etched on the upper side of the substrate and fed through a wide microstrip feedline with a slotted ground plane. Furthermore, the left slot $g2$ in the ground plane is responsible for higher frequencies, and the stub with length $g3$ is responsible for the enhancement of lower frequency. The two L-shaped slots and a small rectangular shape on the ground plane are responsible for CP. Simulation studies are done on Computer Simulation Technology (CST) software, and all the optimized parameters of the designed antenna are shown in Table 1.

Table 1. Geometric Parameters of the proposed antenna.

Parameters	Values (mm)	Parameters	Values (mm)
W	25	L	25
$S1$	11	$g1$	8.5
$S2$	15.8	$g2$	4
$S3$	24	$g3$	3
$S4$	7.5	$g4$	6
$S5$	10.5	$g5$	0.6
$S6$	7	$g6$	11
$S7$	3	$g7$	4.4
$S8$	2.5	h	1.02

The different steps to explain the design procedure of the proposed antenna are shown in Fig. 2. A modified F-shaped structure is placed along with the micro-strip feed line of 22 mm. The modified rectangular structure is opened on one side. Rectangular patches surrounding the fed-line of antenna

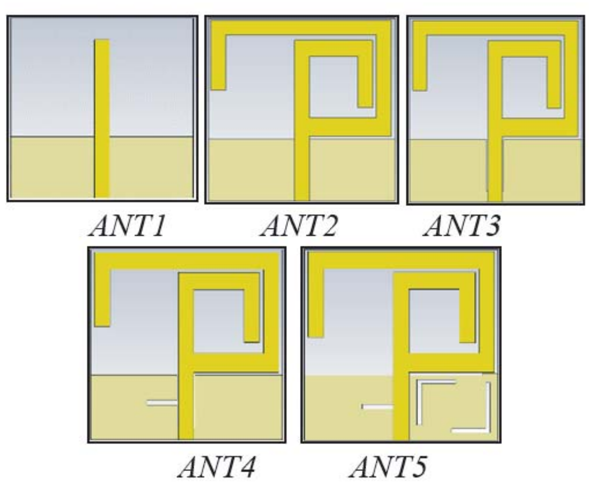

Figure 2. Improvement procedure for designed antenna.

show radiations in free space, and its wavelength refers to the central frequency of the operating bandwidth. The length of the modified rectangular structure and slots in the ground plane varies differently to make it resonate nearly on fundamental mode. To further broaden the ARBW within the IBW, the shape is enhanced more by adding a slot in the ground plane ($g6$).

The ground plane plays an important role in the electromagnetic radiation in all the bands, and this is because of the compactness of the antenna. However, ARBW is largely widened in Ant. 5 by adding perturbation technique in ground plane ($g3$) which affects the current distribution by enhancing CP of the antenna by generating the two orthogonal modes with equal amplitudes and quadrature-phase difference required for CP. Hence, the proposed antenna resonates at three bands that are 8.2% (2.4–2.58 GHz), 33% (3.2–3.9 GHz), and 41.1% (5.2–7.8 GHz). The magnitude of S_{11} parameter shows how much power is radiated from the antenna, shown in Fig. 3(a). This shows that the proposed antenna exhibits good impedance matching on these bands. For the circular polarization antenna, the axial ratio value must be less than 3 dB, shown in Fig. 3(b).

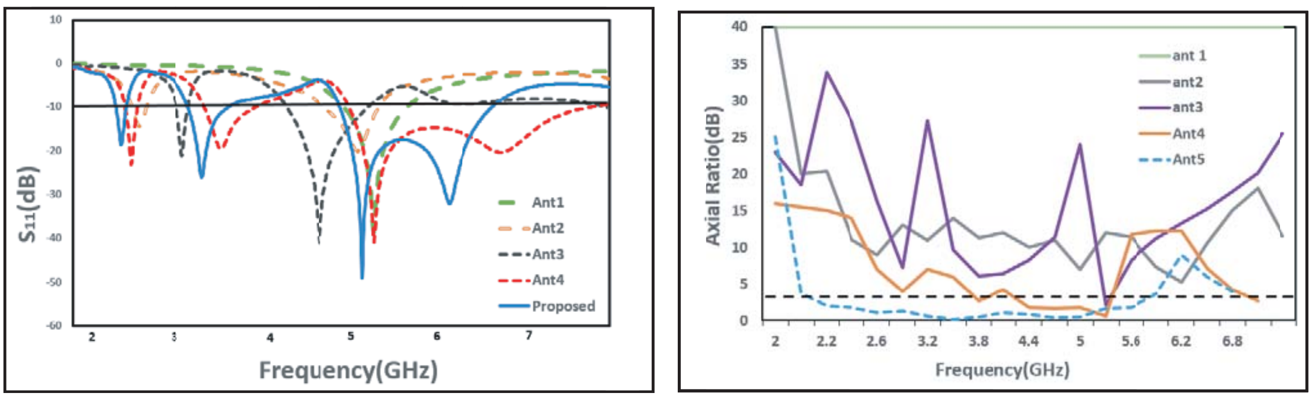

(a) (b)

Figure 3. Simulated results of antenna different steps. (a) S_{11}. (b) Axial ratio.

2.1. Circular Polarization Generation Mechanism

The surface current distribution of the proposed antenna is further studied for illustrating the CP mechanism. Fig. 4 shows the current distribution pattern at 5.2 GHz with the phases of 0°, 90°, 180°, and 270°. It is noted that the maximum current is obtained on the right arm of the parasitic strip ($s2$) and left most arm with the length of $s4$ of the parasitic patch. At initial time $\omega t = 0°$, the current moves in $-x$-direction, and the dominant current flows in the y-direction. When $\omega t = 90°$, the dominant current flows in $+x$ direction. After the next quarter-period, the currents flow in the $+x$ direction.

Finally, at $\omega t = 270°$, the currents are directed in $-y$-direction. In the ground plane, the maximum current is seen in the top right side of the stub having g3 and in slot g2. The magnitudes of current distributions in Figs. 4(a) and 4(c) are almost the same but oppositely directed for Figs. 4(b) and 4(d). It specifies that the direction of the current is counter-clockwise. This describes a left-hand circular polarization (LHCP) pattern when being observed from the $+z$ direction. Right-hand circular polarization (RHCP) is attained by simply mirroring the antenna about the y-z plane.

3. NUMERICAL ANALYSIS FOR THE ANTENNA

To get a better performance, a parametric study is performed. The effect of parameters on the performance of the designed antenna is described in this section. For this purpose, one parameter is varied while others are reserved constant. The parameters $s4$ and $s6$ (patch lengths) and $g1$ and $g2$ (ground slot lengths) are varied alternatively, and their effects are observed on the S_{11} parameter and CP bands.

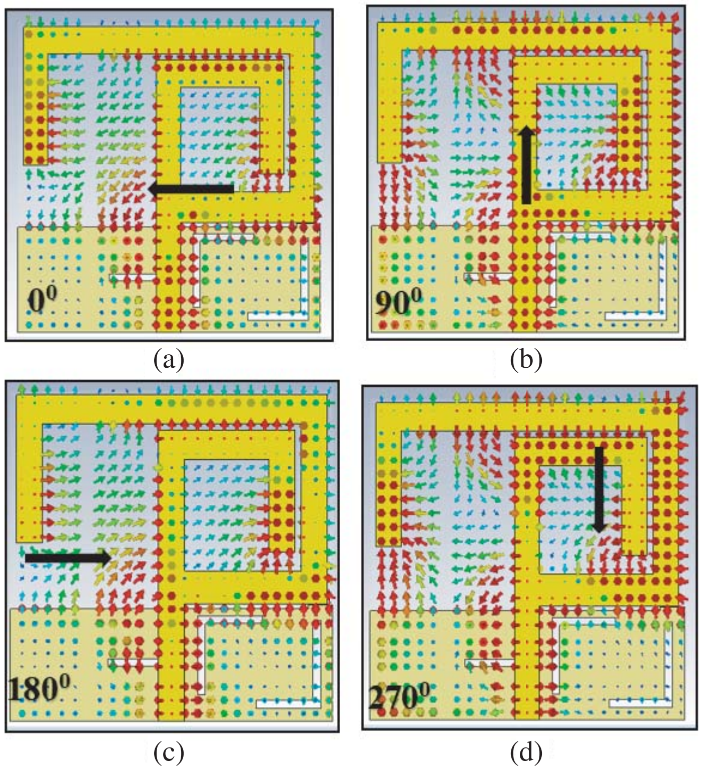

Figure 4. Surface current density over the proposed antenna at 5.2 GHz with the phase of 0°, 90°, 180° and 270°.

3.1. Effects of Length of the Parasitic Strip ($s4$)

The first parameter studied is the left rectangular strip $s4$ in the radiating patch. Its value is varied from 7 to 10 mm while keeping other parameters constant. Fig. 5(a) shows the effect of length on bandwidth. This causes a little effect on bandwidth on the first and last bands by slightly changing the resonating frequency values. When the value of the rectangular strip increases, it improves the return loss as well. This shows that $s4$ is 9 mm which is the suitable value to achieve better ARBW shown in Fig. 5(b).

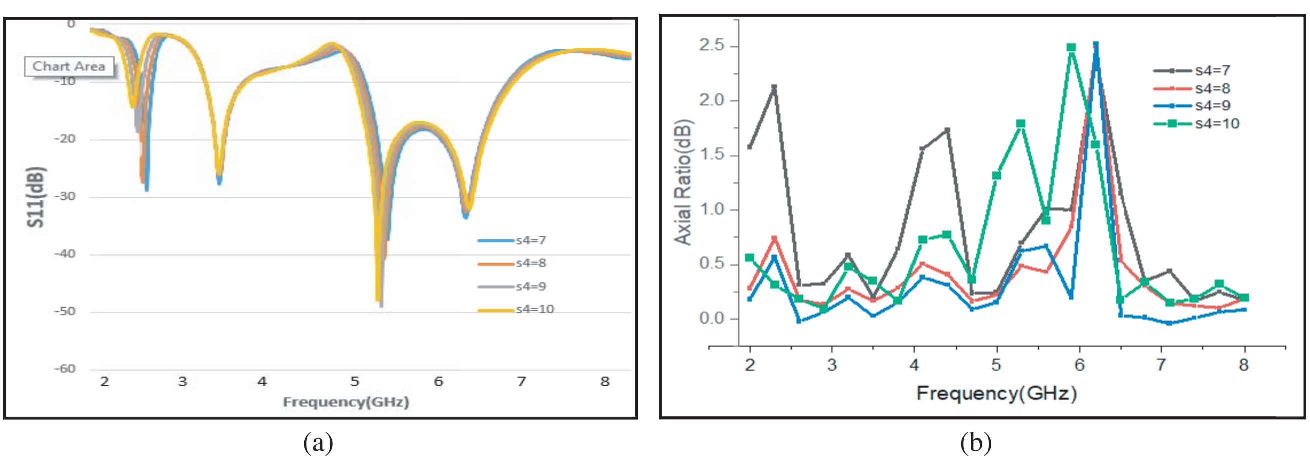

Figure 5. Effects of s4 on antenna performances. (a) S_{11} and (b) axial ratio.

3.2. Effects of the Slot of Ground ($g3$)

The next parameter is the ground slot $g3$, which is varied from 2 to 4 mm. The simulated results due to variation in ground slot are shown in Fig. 6. The slot has a great influence on bandwidth, which is shown in Fig. 6(a). The influence of the AR value is the same as the previous results of $s4$.

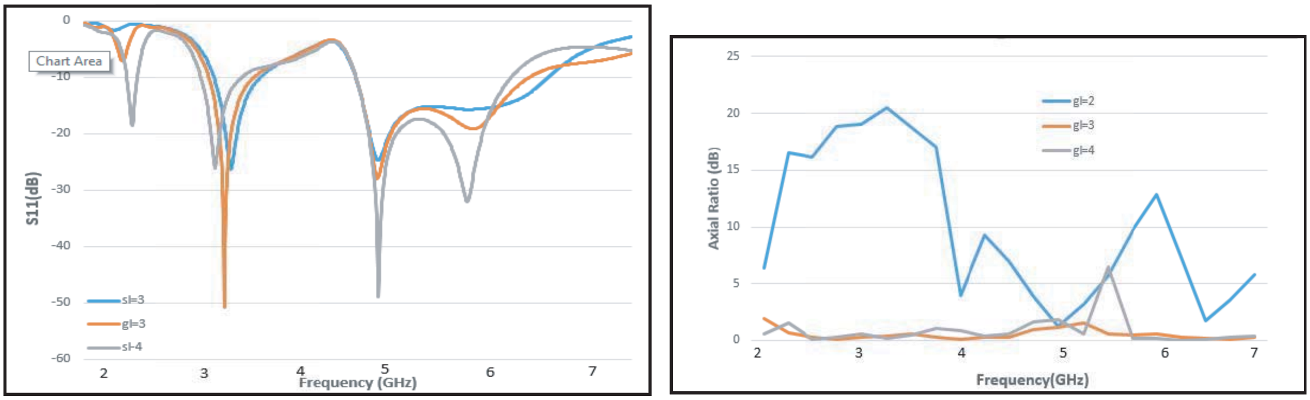

(a) (b)

Figure 6. Effects of $g1$ on antenna performances. (a) S_{11} and (b) axial ratio.

3.3. Effects of Ground Slot Length ($g2$)

The next parameter is the ground slot ($g2$). The increase in the length of slot $g2$ form 4 mm mainly affects the return loss as shown in Fig. 7(a). By increasing the length of the slot, the return loss becomes less. The length of 4 mm is a better value to get results that are more appropriate in all bands. However, when the value of $g2$ is increased to 4 mm, the CP performance of the higher frequency band is little depreciated as shown in Fig. 7(b).

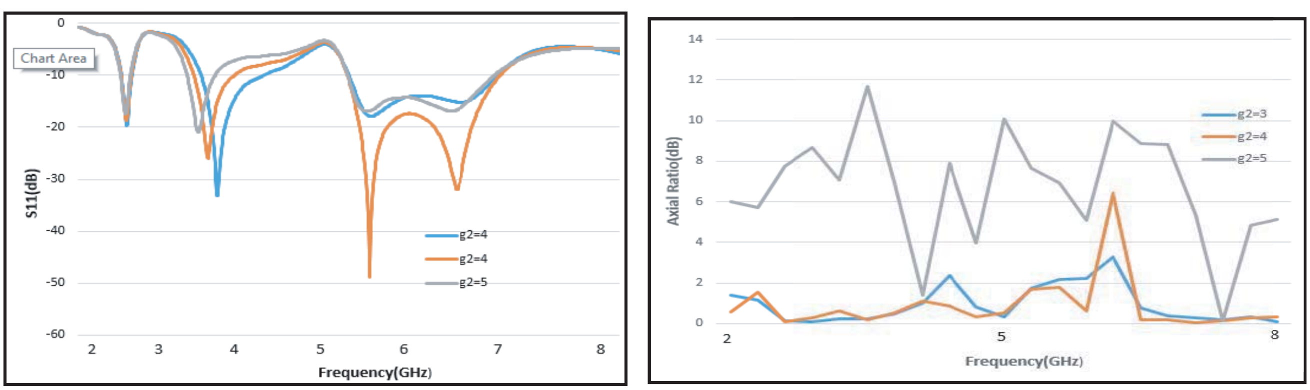

(a) (b)

Figure 7. Effects of $g2$ on antenna performances. (a) S_{11} and (b) axial ratio.

3.4. Effect of Parasitic Strip $s6$

The next parameter is the length of parasitic strip $s6$. The variation of length is from 6 mm to 8 mm (with difference of 1), and it mainly affects the return loss of lower frequency and higher frequency as shown in Fig. 8(a). By increasing the length of the strip, the return loss increases and gets better results at 7 mm, but with again increase of length at 8 mm, return loss is affected, and the CP performance of the antenna is also affected as shown in Fig. 8(b).

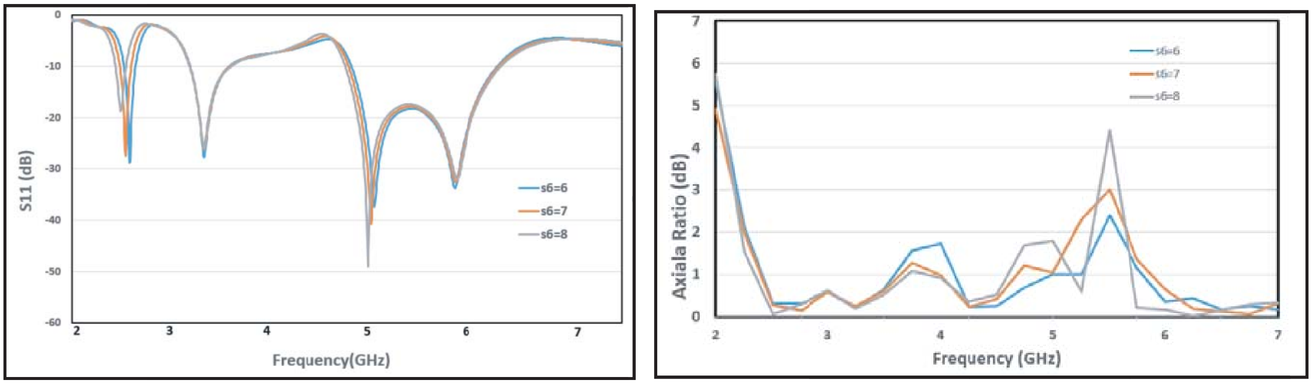

(a) (b)

Figure 8. Effect of $s6$ on (a) S_{11}, (b) axial ratio.

4. EXPERIMENTAL RESULTS

A prototype of the designed antenna is manufactured and shown in Fig. 9. Enhanced measurements are chosen to make the antenna prototype. The designed antenna is fabricated and then tested. The antenna results are measured to verify the simulated ones. The reflection coefficient value is measured with the E8361 Agilent network analyzer. The simulated and measured reflection coefficients graphs of the antenna are depicted in Fig. 10(a). The measured -10 dB reflection coefficient bandwidths are 2.4–2.7 GHz (17.2%) in the lower band, 3.2–3.9 GHz (33%) in the middle band, and 5.2–7.8 GHz (41.1%) in the higher band. The simulated and measured ARs of the proposed antenna are shown in Fig. 10(b). The overlapping -10 dB reflection coefficient and AR bandwidth cover the WLAN, Bluetooth, WiMAX, and Wi-Fi bands. A good agreement is observed between simulated and measured results. Small inconsistencies between measured and simulated results may be observed due to some limitations in fabrication and cable effects. The radiation and gain are tested in an anechoic chamber. The gain of the proposed antenna is 3.5 dB. The antenna achieves wider 3 dB AR bandwidth, which can cover the 5.2/5.8 GHz WLAN, 5.5 GHz Wi-Fi, 2.5/5.5 GHz WiMAX, and ISM 5.8 GHz bands. However, the gain of the antenna in the lower band is less, but it can also be acceptable in modern wireless communication applications. The gain performance of the proposed antenna is shown in Fig. 10(b). The peak gain lies between 0.4 and 3.5 dBi that is achieved over the entire CP band. The radiated efficiency of the proposed antenna is nearly 85% as shown in Fig. 11. It is observed that at low frequencies efficiency is low, but at higher frequency 5–6 GHz, the efficiency of the antenna increases. Simulated radiation

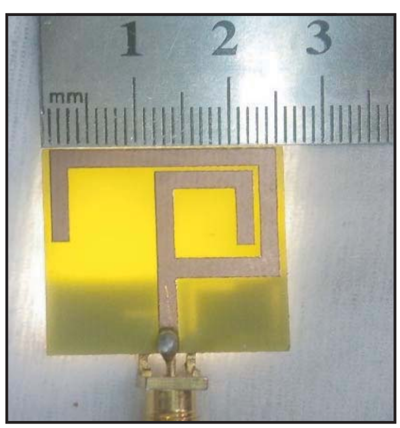

Figure 9. Prototype of proposed antenna.

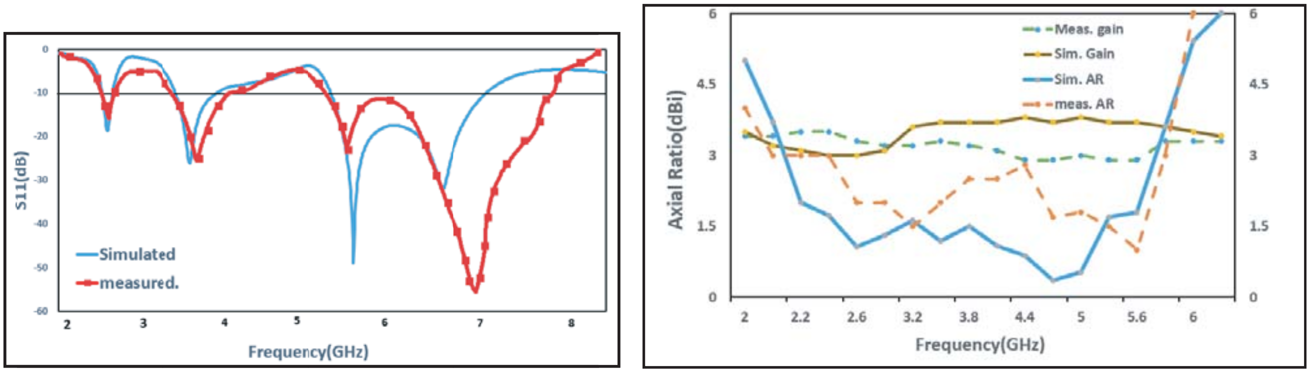

(a) (b)

Figure 10. Simulated and measured results. (a) $|S_{11}|$. (b) AR and realized gain at $\theta = \phi = 0°$.

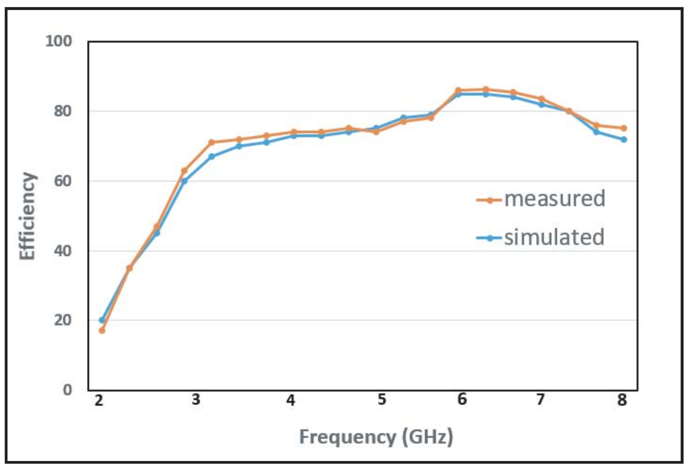

Figure 11. Radiated efficiency of proposed antenna.

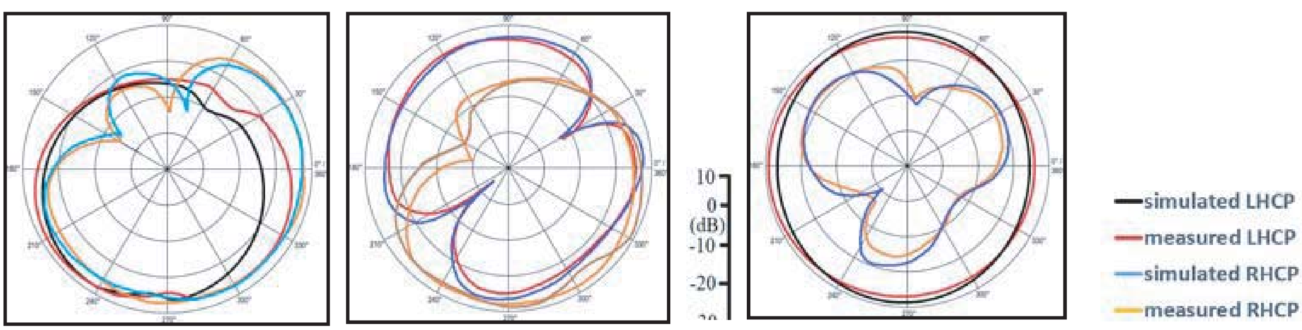

(a) (b) (c)

Figure 12. Radiation Pattern at (a) at 2.45 GHz, (b) at 3.8 GHz, (c) at 5.8 GHz.

patterns of the proposed antenna are in XZ ($\varphi = 0°$) and YZ ($\varphi = 9°$). The proposed antenna radiates RHCP in positive z direction and LHCP in the opposite side of the ground plane that is negative z direction. Fig. 12 shows the radiation pattern at 2.4, 3.8, and 5.8 GHz frequencies.

The comparison between the designed antennas and the previous antennas is shown in Table 2 that includes the size of the antenna, IBW, 3 dB ARBW, and gain. It is deduced that the proposed antenna

Table 2. Comparison between proposed antennas and similar ones in literature review.

Ref.	Size (mm^3)	Band	Impedance BW	Axial ratio (ARBW)	Gain (dBi)
[5]	$30 \times 32 \times 1.6$	WLAN applications	62.94% (3.92–7.52 GHz)	53.92% 4.28–7.44 GHz	3.2
[6]	$50 \times 60 \times 1.6$	GPS and SDAR bands	1.45 to 3.93 GHz	4.15% 65 MHz 4.55% 107 MHz	4.3
[8]	$42 \times 48.4 \times 1.6$	WLAN, Wi-Fi, Bluetooth, WiMAX	2.38–2.75 GHz 4.05–6.38 GHz	1.43% 2.39–3 GHz 1.65% 5.15–6 GHz	3.9
[9]	$60 \times 60 \times 1$	WLAN bands and Some X-band applications	44.0%, 2.34–3.66 GHz 70.9%, 4.55–9.55 GHz	35.9% 2.40–3.45 GHz 44.0% 4.65–7.27 GHz 6.3% 8.13–8.66 GHz	3.5
[10]	$25 \times 35 \times 1.6$	WLAN, WiFi and WiMAX	9.7% (2.05–2.26) GHz 11.3% (3.41–3.82 GHz), 60.2% (4.89–9.11 GHz)	4.9% 3.53–3.71 GHz 58.6% 4.69–8.58 GHz	4.2
[11]	$30 \times 30 \times 1.6$	WiMAX, WLAN, ISM	92.6% (5 GHz, 2.9–7.9 GHz)	83.5% 3–7.3 GHz	3.18
[12]	$28 \times 28 \times 1.6$	WiMAX, WLAN	84% 3.25–8.0 GHz	41.3% 4.4–6.67 GHz	3.5
[13]	$44 \times 44 \times 1.6$	ISM, WiMAX, WLAN, satellite communications	56%, (2.25–4.0 GHz)	63.61%, 2.38–4.60 GHz	2.08
Prop.	$25 \times 25 \times 1.02$	WiMAX and WLAN, WiFi, Bluetooth, UMTS, ISM, GSM	8.2% (2.4–2.58 GHz), 33% (3.2–3.9 GHz), and 41.1% (5.2–7.8 GHz)	89.7% (2.17–5.8 GHz)	3.5

has the advantage of compact size and widest ARBW with slotted structure. The slight divergences are accredited to that some manufacturing effects might be in SMA connector and the returning currents on the shield of the feeding cable which is the basis of some agitations in the pattern.

5. CONCLUSION

A broadband CP monopole, planar geometry antenna with wide AR is proposed with a simple and compact structure having dimensions of $25 \times 25 \times 1.02\,\text{mm}^2$. A modified F-shaped parasitic patch and slotted ground plane antenna is proposed to enhance ARBW. The IBWs of the proposed antenna are 8.2% (2.4–2.58 GHz), 33% (3.2–3.9 GHz), and 41.1% (5.2–7.8 GHz). Achieved 3-dB axial ratio bandwidth is 89.7% (2.17–5.8 GHz). Furthermore, the gain of antenna is also improved for multiband applications. The proposed antenna is capable of getting service for WiMAX WLAN, Bluetooth, WI-Fi, and ISM applications.

ACKNOWLEDGMENT

The authors would like to thank the National University of Sciences and Technology, Islamabad, Pakistan for supportive work in obtained the information and material in the development for our work. Also Thanks to the nameless referees, lecturers and other researchers, whose explanations, consultation and observation led to an enhanced appearance of our projects.

REFERENCES

1. Zaker, R. and A. Abdipour, "A very compact ultrawideband printed omnidirectional monopole antenna," *IEEE Antennas and Wireless Propagation Letters*, Vol. 9, 471–473, 2010.
2. Rocca, P., M. Donelli, G. Oliveri, F. Viani, and A. Massa, "Reconfigurable sum-difference pattern by means of parasitic elements for forward-looking monopulse radar," *IET Radar, Sonar and Navigation*, Vol. 7, No. 7, 747–754, 2013.
3. Shin, Y. S., S. O. Park, and M. Lee, "A broadband interior antenna of planar monopole type in handsets," *IEEE Antennas and Wireless Propagation Letters*, Vol. 4, 9–12, 2005.
4. Foudazi, A., H. R. Hassani, and S. M. A. Nezhad, "Small UWB planar monopole antenna with added GPS/GSM/WLAN bands," *IEEE Transactions on Antennas and Propagation*, Vol. 60, No. 6, 2987–2992, 2012.
5. Midya, M., S. Bhattacharjee, and M. Mitra, "Broadband circularly polarized planar monopole antenna with G-shaped parasitic strip," *IEEE Antennas and Wireless Propagation Letters*, Vol. 18, No. 4, 581–585, 2019.
6. Wang, C.-J., M.-H. Shih, and L.-T. Chen, "A wideband open-slot antenna with dual-band circular polarization," *IEEE Antennas and Wireless Propagation Letters*, Vol. 14, 1306–1309, 2015.
7. Ellis, M. S., et al., "A novel simple and compact microstrip-fed circularly polarized wide slot antenna with wide axial ratio bandwidth for C-band Applications," *IEEE Transactions on Antennas and Propagation*, Vol. 64, No. 4, 1552–1555, 2016.
8. Li, Q., et al., "Dual-band circularly polarised planar monopole antenna for WLAN/Wi-Fi/Bluetooth/WiMAX applications," *IET Microwaves, Antennas & Propagation*, Vol. 12, No. 6, 972–976, 2017.
9. Xu, R., et al., "A design of triple-wideband triple-sense circularly polarized square slot antenna," *IEEE Antennas and Wireless Propagation Letters*, Vol. 16, 1763–1766, 2017.
10. Gyasi, K. O., et al., "Tri-band planar monopole antenna with two circularly polarised bandwidths for WiMAX applications," *IET Microwaves, Antennas & Propagation*, Vol. 12, No. 15, 2350–2355, 2018.
11. Gyasi, K. O., et al., "A compact broadband circularly polarized slot antenna with two linked rectangular slots and an inverted-F feed line," *IEEE Transactions on Antennas and Propagation*, Vol. 66, No. 12, 7374–7377, 2018.
12. Nosrati, M. and N. Tavassolian, "Miniaturized circularly polarized square slot antenna with enhanced axial-ratio bandwidth using an antipodal Y-strip," *IEEE Antennas and Wireless Propagation Letters*, Vol. 16, 817–820, 2016.
13. Yeung, S. H., K. F. Man, and W. S. Chan, "A bandwidth improved circular polarized slot antenna using a slot composed of multiple circular sectors," *IEEE Transactions on Antennas and Propagation*, Vol. 59, No. 8, 3065–3070, 2011.
14. Naser-Moghadasi, M., R. Sadeghzadeh, L. Asadpor, et al., "A small dual band CPW-fed monopole antenna for GSM and WLAN applications," *IEEE Antennas and Wireless Propagation Letters*, Vol. 12, 508–511, 2013.
15. Jan, J.-Y., C.-Y. Pan, K.-Y. Chiu, and H.-M. Chen, "Broadband CPW-fed circularly polarized slot antenna with an open slot," *IEEE Transactions on Antennas and Propagation*, Vol. 61, No. 3, 1418–1422, Mar. 2013.
16. Samsuzzaman, Md, M. T. Islam, and M. J. Singh, "A compact printed monopole antenna with wideband circular polarization," *IEEE Access*, Vol. 6, 54713–54725, 2018.

17. Mousavi, P., B. Miners, and O. Basir, "Wideband L-shaped circular polarized monopole slot antenna," *IEEE Antennas and Wireless Propagation Letters*, Vol. 9, 822–825, 2010.
18. Rezaeieh, S. A., A. Abbosh, and M. Antoniades, "Compact CPW-fed planar monopole antenna with wide circular polarization bandwidth," *IEEE Antennas and Wireless Propagation Letters*, Vol. 12, 1295–1298, 2013.
19. Chen, X., L. Wang, D. Wu, J. Lei, and G. Fu, "Compact and wideband directional circularly polarized distributed patch antenna with high efficiency," *IEEE Access*, Vol. 5, 15942–15947, 2017.
20. Liang, W. L., Y. C. Jiao, Y. C. Luan, et al., "A dual-band circularly polarized complementary antenna," *IEEE Antennas and Wireless Propagation Letters*, Vol. 14, 4, 2015.
21. Verma, A., et al., "A compact circularly polarized modified printed monopole antenna for wireless applications," *Electromagnetics*, Vol. 40, No. 8, 576–593, 2020.
22. Jaiverdhan, M. M. Sharma, R. P. Yadav, and R. Dhara, "Characteristic mode analysis and design of broadband circularly polarized CPW-fed compact printed square slot antenna," *Progress In Electromagnetics Research M*, Vol. 94, 105–118, 2020.
23. Sankhla, V. and A. Kumar, "An offset CPW-fed dual-band circularly polarized printed antenna for multiband wireless applications," *Optical and Wireless Technologies*, 411–418, Springer, Singapore, 2020.
24. Robol, F. and M. Donelli, "Circularly polarized monopole hook antenna for ISM-band systems," *Microwave and Optical Technology Letters*, Vol. 60, No. 6, 1452–1454, June 2018.
25. Donelli, M. and P. Febvre, "An inexpensive reconfigurable planar array for Wi-Fi applications," *Progress In Electromagnetics Research C*, Vol. 28, 71–81, 2012.
26. Donelli, M., T. Moriyama, and M. Manekiya, "A compact switched-beam planar antenna array for wireless sensors operating at Wi-Fi band," *Progress In Electromagnetics Research C*, Vol. 83, 137–145, 2018.
27. Donelli, M., T. Moriyama, and M. Manekiya, "A compact switched-beam planar antenna array for wireless sensors operating at Wi-Fi band," *Progress In Electromagnetics Research C*, Vol. 83, 137–145, 2018.